The decomposition of peroxynitrite to nitroxyl anion (NO^-) and singlet oxygen in aqueous solution

Ahsan Ullah Khan*†, Dianne Kovacic*, Alexander Kolbanovskiy*, Mehul Desai‡, Krystyna Frenkel‡, and Nicholas E. Geacintov*

*Department of Chemistry, New York University, New York, NY 10003; and †Department of Environmental Medicine, New York University, New York, NY 10016

Communicated by Michael Kasha, Florida State University, Tallahassee, FL, December 31, 1999 (received for review November 22, 1999)

The mechanism of decomposition of peroxynitrite ($OONO^-$) in aqueous sodium phosphate buffer solution at neutral pH was investigated. The $OONO^-$ was synthesized by directly reacting nitric oxide with superoxide anion at pH 13. The hypothesis was explored that $OONO^-$, after protonation at pH 7.0 to HOONO, decomposes into $^1O_2$ and HNO according to a spin-conserved unimolecular mechanism. Small aliquots of the concentrated alkaline $OONO^-$ solution were added to a buffer solution (final pH 7.0–7.2), and the formation of $^1O_2$ and NO^- in high yields was observed. The $^1O_2$ generated was trapped as the transannular peroxide ($DPAO_2$) of 9,10-diphenylanthracene (DPA) dissolved in carbon tetrachloride. The nitroxyl anion (NO^-) formed from HNO (pKa 4.5) was trapped as nitrosylhemoglobin (HbNO) in an aqueous methemoglobin (MetHb) solution. In the presence of 25 mM sodium bicarbonate, which is known to accelerate the rate of decomposition of $OONO^-$, the amount of singlet oxygen trapped was reduced by a factor of ≈2 whereas the yield of trapping of NO^- by methemoglobin remained unaffected. Because NO_3^- is known to be the ultimate decomposition product of $OONO^-$, these results suggest that the nitrate anion is not formed by a direct isomerization of $OONO^-$, but by an indirect route originating from NO^-.

nitrosylhemoglobin | diphenylanthracene endoperoxide

Peroxynitrite is a potent oxidant formed by the near diffusion-controlled reaction of nitric oxide ($NO^\bullet$) and superoxide ion (O_2^-) (1). Both nitric oxide and superoxide are produced by activated macrophages (2, 3), neutrophils (4), and endothelial cells (5, 6). There is evidence that peroxynitrite is formed in significant concentrations *in vivo* (7–9) and may contribute to an increased risk for cancer (10), artherosclerosis (11), stroke (12), and other diseases (13). Peroxynitrite is a stable anion in alkaline solution (pKa of 6.8); however, once protonated, it decomposes rapidly with a half-life of less than 1 s at physiological pH at 37°C (14), generating reactive species that readily react with biomolecules such as lipids (15), amino acids (16), and DNA (17). Central to the question of the biochemistry of peroxynitrite is the mechanism of decomposition and the identity of the reactive species, a subject of intense research and controversy (18–21). Speculations about the decomposition mechanisms are largely based on kinetic and thermodynamic considerations (22). It has been shown that bicarbonate ion enhances the rate of disappearance of peroxynitrite, leading to the proposal of a nitrosoperoxycarbonate anion adduct, with a distinctly different chemistry from that of $OONO^-$ (19).

We reported previously that the mere acidification of an aqueous peroxynitrite solution resulted in chemiluminescence at 1,270 nm characteristic of the deactivation of singlet oxygen (23). By comparing the intensity of this emission to that of $^1O_2$ generated by the reaction of hydrogen peroxide (H_2O_2) with hypochlorite anion (OCl^-), which is known to be stoichiometric (24), it was concluded that the yield of $^1O_2$ from peroxynitrite was nearly stoichiometric. These results suggested a spin-conserved process leading to the generation of $^1O_2$ from peroxynitrite. However, the highly exothermic neutralization reaction of the acidic with the basic reactant and the local non-equilibrium conditions made extrapolating this interpretation to biological conditions at pH 7 uncertain. We decided to examine the nature of the reactive species generated in the decomposition of peroxynitrite under more controlled and physiologically relevant conditions.

In this communication we report an important reaction pathway for the decomposition of peroxynitrite that yields two transient species, nitroxyl anion (NO^-) and singlet molecular oxygen. By using well established analytical procedures, an aqueous alkaline solution (pH ≈13) of peroxynitrite was allowed to react in separate but parallel experiments with two chemical traps, one specific for singlet oxygen and one specific for the nitroxyl anion, NO^-. Singlet oxygen was trapped as the transannular peroxide ($DPAO_2$) of 9,10-diphenylanthracene (DPA) (25–27), and the nitroxyl anion was trapped as nitrosylhemoglobin (HbNO) in aqueous solutions of methemoglobin (MetHb) (28), both with very high yields. The effects of bicarbonate ions on the yields of NO^- and $^1O_2$ in aqueous solution were investigated.

Methods

Chemicals. Bovine MetHb (Sigma) was crystallized, dialyzed, and lyophilized. DPA (97%), perylene (99%), 2,3-dimethyl-2-butene [tetramethylethylene (TME)] (98%), acetone (spectral grade), potassium superoxide (KO_2), and potassium hydroxide (KOH) were obtained from Aldrich. Angeli's salt ($Na_2N_2O_3$) was obtained from Cayman Chemicals (Ann Arbor, MI). Hydrogen peroxide (H_2O_2) (30% aqueous solution) (Certified ACS), sodium hypochlorite (NaOCl) (4–6% available chlorine, purified grade), and acetone were from Fisher. Carbon tetrachloride (Reagent ACS) was obtained from Spectrum Chemical (Gardnia, CA), and nitric oxide (NO) gas was from Matheson Gas (East Rutherford, NJ).

Peroxynitrite. Peroxynitrite was generated as described (23) by bubbling NO gas into a deoxygenated 1 M KOH solution at 0°C, and then adding KO_2 powder (≈5 mg), in small amounts, until a bright yellow solution was obtained. The pH of the solution was ≈13, and the concentration of peroxynitrite was in the range of 70–110 mM based on the absorbance at 302 nm (ε = 1,670 $M^{-1}\cdot cm^{-1}$) (29).

Reagent Solutions. A concentrated solution of MetHb was made in 1 ml of deoxygenated 70 mM phosphate buffer (pH 7.0) and

Abbreviations: DPA, 9,10-diphenylanthracene; HbNO, nitrosylhemoglobin; MetHb, methemoglobin; TME, tetramethylethylene.

†To whom reprint requests should be addressed at: 453 Brown Building, Department of Chemistry, New York University, 29 Washington Square, New York, NY 10003. E-mail: ak14@is.nyu.edu.

The publication costs of this article were defrayed in part by page charge payment. This article must therefore be hereby marked "*advertisement*" in accordance with 18 U.S.C. §1734 solely to indicate this fact.

Article published online before print: *Proc. Natl. Acad. Sci. USA*, 10.1073/pnas.050587297. Article and publication date are at www.pnas.org/cgi/doi/10.1073/pnas.050587297

was further purified by passing through a Sephadex G-25 column (Pharmacia) using 70 mM phosphate buffer as the elutant. The eluted solution was then diluted with additional 70 mM phosphate buffer to bring the concentration to around 60–85 μM. The concentration was determined by absorbance at 406 nm ($\varepsilon_{406} = 154\ mM^{-1}\cdot cm^{-1}$) (30). Solutions of $Na_2N_2O_3$ (80 mM) in 10 mM NaOH were prepared just before use and were stored on ice. Solutions of KNO_2 (100 mM) were prepared in 70 mM phosphate buffer (pH 7.0). Solutions of $NaHCO_3$ were prepared by adding premeasured amounts of solid sodium bicarbonate, to give a final concentration of 25 mM (31), to individual polypropylene centrifuge tubes, to which were added 2-ml aliquots of the MetHb solutions in 70 mM phosphate buffer.

NO^- Trapping by MetHb Under N_2. Experimental procedures were as follows: First, aliquots were taken from an individual sample of the 2 ml of buffered 80 μM MetHb solution (with or without sodium bicarbonate), absorption spectra were taken with either a 1-mm path length cuvette for the 400-nm Soret region or 1-cm for the visible region. Next, the solutions were transferred back to the centrifuge tube. To this MetHb solution was then added one aliquot (from 1 to 10 μl) of either peroxynitrite or KNO_2 solution, or KOH solution, immediately before the absorption spectrum was recorded. The absorption spectrum of the MetHb/$Na_2N_2O_3$ solution was recorded 10 min after addition, resulting in the HbNO reference spectrum (without bicarbonate). Absorption measurements were made by using a Hewlett Packard 8453 UV-VIS diode array spectrophotometer. After the absorption measurements, the pH of each of the solutions was measured with a pH meter (Horizon Ecology, Chicago).

Trapping of $^1O_2$. In a typical biphasic experiment, 0.50 ml CCl_4 solutions containing either 80 mM DPA and 0.8 mM perylene (solution **A**), or 80 mM DPA, 0.8 mM perylene, and 80 mM TME (solution **B**), were pipetted into 15-ml propylene centrifuge tubes; 100-μl aliquots of 75 mM $OONO^-$ solution (pH 13) were then pipetted on top of the CCl_4 layer, and the two layers were mixed thoroughly by vortexing. While continuing the vortexing, a total of 5 ml of 20 mM phosphate buffer (pH 7) (with or without bicarbonate) were added drop-wise to this emulsified CCl_4 solution to initiate the decomposition of peroxynitrite. After separation of the layers, the aqueous layer was discarded, and the procedure was repeated, using 100-μl aliquots of the $OONO^-$ solution, until the 2-ml aliquot of the peroxynitrite solution was used up. The CCl_4 layer was then washed twice with 10 ml of distilled water. The CCl_4 solution was then evaporated to dryness under vacuum. The residue was dissolved in 2 ml of acetone, and 50-μl aliquots were analyzed by HPLC techniques. The HPLC system consisted of a Waters Model 510 solvent delivery system with an SPD-10A UV-Vis detector (Shimadzu) employing a 250- $\times$ 10-mm C18 Hypersil 5 column (Phenomenex, Belmont, CA), and a linear gradient 30–100% (60 min) of acetonitrile in water (flow rate 2 ml/min, UV detection of products at 210 nm).

Estimation of Singlet Oxygen Yields from Peroxynitrite Decomposition. The amount of $^1O_2$ generated from the decomposition of $OONO^-$ was estimated by comparing the yield of formation of the endoperoxide $DPAO_2$ (25) to the yield of $DPAO_2$ resulting from $^1O_2$ generated by the extensively studied reaction of H_2O_2 with NaOCl under comparable conditions. Both H_2O_2 (30%, 12.5 M) and NaOCl ($\approx$0.7 mM) were diluted with 1 M KOH solution to $\approx$75 mM (which is equivalent to the peroxynitrite concentration of 75 mM used in parallel experiments). A total of 2 ml of 75 mM H_2O_2 was reacted with a total of 2 ml of 75 mM NaOCl in the presence of 0.5 ml CCl_4 solutions **A** or **B**. As in the case of the peroxynitrite experiments above, the reactions were carried out stepwise in small batches of 200 μl of 75 mM H_2O_2 and 0.5 ml CCl_4 solution, as described above for the $OONO^-$ decomposition reactions.

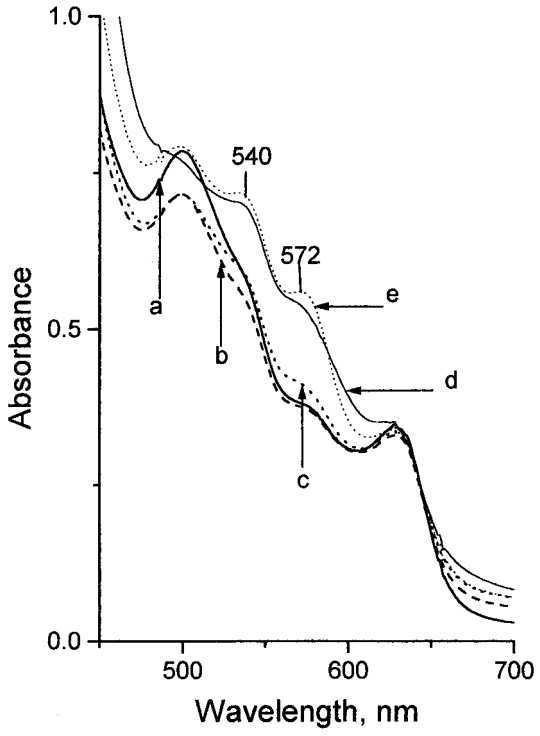

Fig. 1. Methemoglobin conversion to nitrosylhemoglobin. Shown are absorption spectra of solutions of 80 μM MetHb in 70 mM phosphate buffer (pH 7.0) at room temperature under N_2. Trace a, MetHb solution at pH 7.0; trace b, MetHb solution at pH 7.2; trace c, MetHb solution with 100 mM KNO_2; trace d, MetHb solution, equilibrated absorption spectrum measured $\approx$10 s after the addition of 160 μM $ONOO^-$, final pH 7.2; trace e, absorption spectrum of MetHb solution 10 min after the addition of 160 μM Angeli's salt (pH 7.0).

Results

Trapping of NO^- from Peroxynitrite by MetHb. Nitroxyl anion (NO^-) was trapped by MetHb [Fe(III) state] to produce HbNO [Fe(II) state] under N_2. The conversion of MetHb to HbNO results in the appearance of two new absorption bands at 540 and 572 nm (28). The identification of HbNO generated in the decomposition of peroxynitrite was based on the comparison of these two bands with those obtained from the reaction of MetHb with Angeli's salt ($Na_2N_2O_3$). Angeli's salt, under neutral or mildly alkaline conditions, decomposes via its monoanion, $HN_2O_3^-$, to quantitatively generate NO^-, and is known to efficiently convert MetHb to HbNO as the sole heme product (28).

The MetHb absorption spectra generally depend on the pH of the solution. Therefore, our experiments were performed in a limited pH range of 7.0 to 7.2 (28). In this pH range, the effect of pH on the absorption spectra, particularly in the wavelength region of interest from 535 to 635 nm, is small (Fig. 1, trace a, pH 7.0; trace b, pH 7.2).

In the synthesis of peroxynitrite, nitrate (NO_3^-) and nitrite (NO_2^-) anions are also produced. Of these, NO_3^- does not interfere in the nitroxyl trapping by MetHb (results not shown); NO_2^-, on the other hand, is known to bind to MetHb (32) and could, potentially, interfere in these experiments. However, the absorption spectrum of MetHb in the presence of 100 mM KNO_2 (Fig. 1, trace c) shows that the NO_2^- ions have a negligible effect on the absorption spectrum of MetHb as compared with the effect of $OONO^-$ (Fig. 1, trace d).

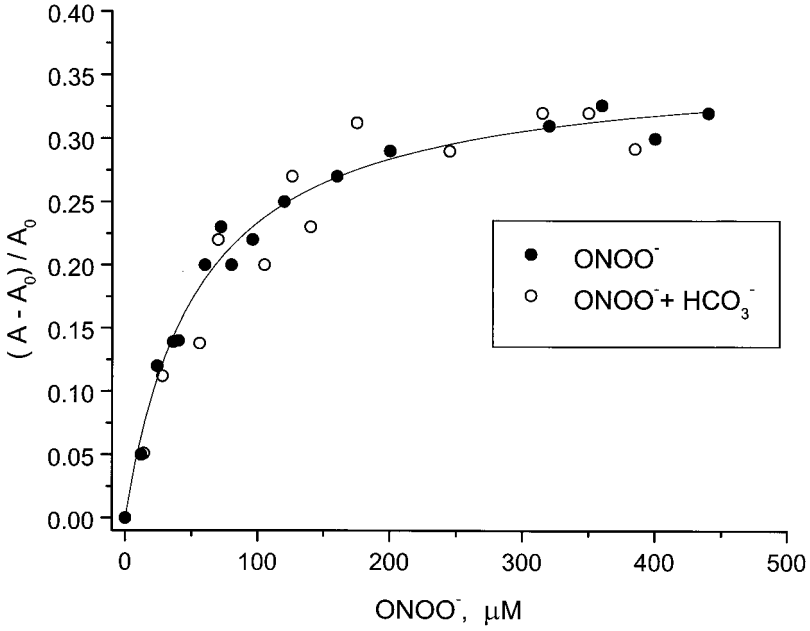

Fig. 2. Change in absorbance (A) at 572 nm of a methemoglobin solution (85 μM) at different initial [$ONOO^-$] concentrations, within ≈10 s of addition of bolus amounts of a concentrated peroxynitrite solution, without (●) and in the presence of a 25 mM sodium bicarbonate solution (○) at pH 7.0–7.2 under a N_2 atmosphere; A_0 is the absorbance at 572 nm in the absence of peroxynitrite. The solid line is a plot of the noncooperative, single-binding-site isotherm $0.36 \times \{[ONOO^-]/([ONOO^-] + K]\}$, with the value of the equilibrium constant $K = 55$ μM.

The spectra of MetHb (80 μM) in the presence of $OONO^-$ (220 μM) and NO^- generated from the decomposition of Angeli's salt (160 μM) are compared in Fig. 1 (traces d and e). In both cases, new bands or shoulders are apparent at 540 and 572 nm that are characteristic of HbNO. These changes in absorbance were complete within the 8- to 10-s manual mixing time.

Peroxynitrite Titration of MetHb in the Presence and Absence of HCO_3^-. Titration of 80 μM MetHb with aliquots of a 100 mM peroxynitrite solution (under 1 atm N_2), thus generating HbNO, was undertaken to determine the binding characteristics of NO^- to MetHb in the absence and the presence of 25 mM sodium bicarbonate in 70 mM sodium phosphate buffer solutions. The concentration of HbNO was monitored by following the absorbance at 572 nm (Fig. 2, closed circles). Saturation of the MetHb binding sites occurs approximately near a 100 μM $OONO^-$ concentration, which is close to a 1:1 MetHb:$OONO^-$ concentration ratio. This is consistent with a dissociation of $OONO^-$ to NO^-, and a near-stoichiometric binding of the latter to MetHb to form the observed HbNO complex. The half-life of the HbNO complex is known to be of the order of hours in the absence of oxygen (32), and therefore its dissociation can be neglected under the conditions of the experiments depicted in Fig. 2. Interestingly, the effect of 25 mM bicarbonate (Fig. 2, open circles) on the extent of HbNO formation is negligible. This observation suggests that bicarbonate ions do not significantly influence the formation of NO^- from $OONO^-$ under the conditions of our experiments (see below).

Trapping of $^1O2$ from Peroxynitrite by Diphenylanthracene. Using an extension of a procedure developed earlier (27), we have identified and quantitated the amount of $^1O_2$ generated in the decomposition of peroxynitrite in the biphasic reaction system described above. In brief, $^1O_2$ reacts rapidly and specifically with DPA ($k_r = 1.3 \times 10^6$ $M^{-1}{\cdot}s^{-1}$) (33) to produce DPA endoperoxide ($DPAO_2$); $DPAO_2$ is stable at room temperature (27). Perylene is used here as an internal standard in the HPLC experiments to provide a means for quantitating the amount of $DPAO_2$ formed (perylene reacts ≈100 times more slowly with $^1O_2$ than DPA) (34). TME reacts with $^1O_2$ to generate a stable hydroperoxide [($k_r = 29.7 \times 10^6$ $M^{-1}{\cdot}s^{-1}$) (33)] and is used here as a competitive inhibitor of DPA peroxidation.

When peroxynitrite (2 ml of a 75 mM $OONO^-$ solution) is allowed to decompose stepwise at pH 7 in the basic aqueous buffer/CCl_4 system (solution **A**), the HPLC elution profile shown in Fig. 3*A* is obtained. This profile shows a prominent peak due to unreacted DPA and a smaller peak due to the $DPAO_2$ endoperoxide product; the area under this trace is ≈30% relative to the area of the perylene standard. In contrast, the $DPAO_2$ fraction is missing entirely when the decomposition of $OONO^-$ takes place in the presence of 78 mM tetramethylethylene, an efficient trap of singlet oxygen (Fig. 3*B*).

The yield of $^1O_2$ from the H_2O_2/OCl^- reaction in aqueous buffer solution occurs with ≈100% efficiency as reported by Held *et al.* (24). We therefore compared the yields of $^1O_2$, as measured by the appearance of $DPAO_2$, from the $OONO^-$ decomposition and the H_2O_2/OCl^- using the same concentrations of reactants in both cases. The HPLC elution profile derived from a positive control experiment in which $^1O_2$ is generated by the well characterized H_2O_2/OCl^- reaction that generates $^1O_2$ is shown in Fig. 3*C*. As expected, a fraction attributed to $DPAO_2$ is apparent (≈25% of the perylene integrated peak area). Fig. 3*D* shows an elution profile of a fraction derived from another H_2O_2/OCl^- reaction identical to the one shown in *C*, except that the $^1O_2$ scavenger TME (78 mM) was also present; as expected, the $DPAO_2$ fraction is missing in *D*. The normalized yields of $^1O_2$, as measured by the $DPAO_2$/perylene ratios, are comparable to one another in these two experiments, suggesting a high efficiency of formation of $^1O_2$ from $OONO^-$.

Yield of $^1O_2$ from $OONO^-$ in the Presence of 25 mM Sodium Bicarbonate. The effect of sodium bicarbonate on the $^1O_2$ yield from the $OONO^-$ decomposition and the H_2O_2/OCl^- reactions, as mea-

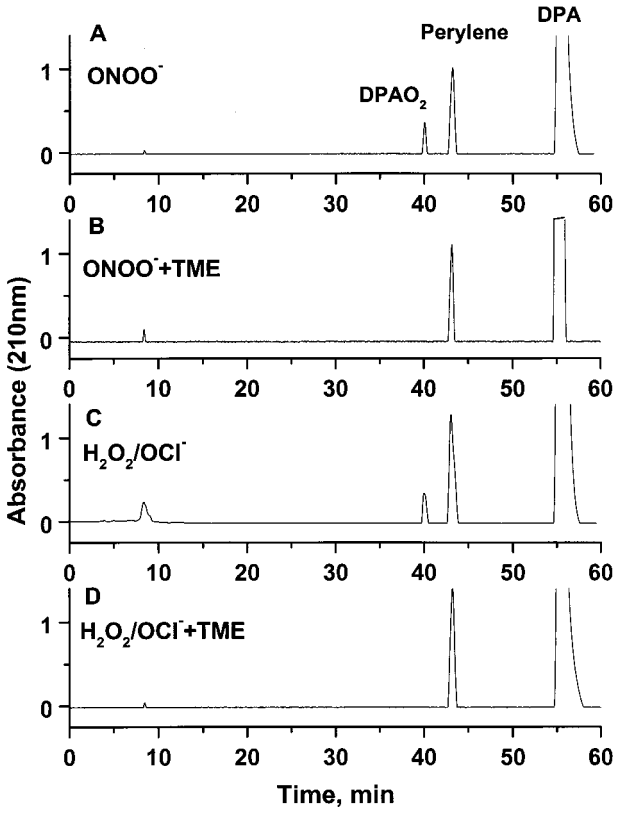

Fig. 3. Diphenylanthracene (DPA) trapping of $^1O_2$ as diphenylanthracene endoperoxide ($DPAO_2$) in a CCl_4 layer after the decomposition of $ONOO^-$ in an aqueous layer in a biphasic system (see *Methods*). These reactions were carried out with and without the $^1O_2$ trap TME in the CCl_4 layer. Perylene was present in the CCl_4 layers at constant concentrations in all of the experiments, and served as an internal standard. (*A*) Stepwise decomposition of $ONOO^-$ in the aqueous layer in the absence of TME in the CCl_4 layer (solution **A**; see *Methods*); the HPLC elution profile exhibits three fractions, each representing unreacted DPA, perylene, and $DPAO_2$, respectively. *B* shows the result of an analogous decomposition experiment as in *A*, but with 78 mM TME in the CCl_4 layer (solution **B**; see *Methods*). *C* is the elution profile of a positive control in which $^1O_2$ was generated from the highly efficient H_2O_2/OCl^- reaction in the aqueous layer (solution **A**). *D* shows the result obtained after an experiment analogous to the one in *C*, except that the CCl_4 solution contained 78 mM TME (solution **B**). The results shown in *C* can be used to estimate the amount of $^1O_2$ generated in the decomposition of $ONOO^-$, shown in *A*.

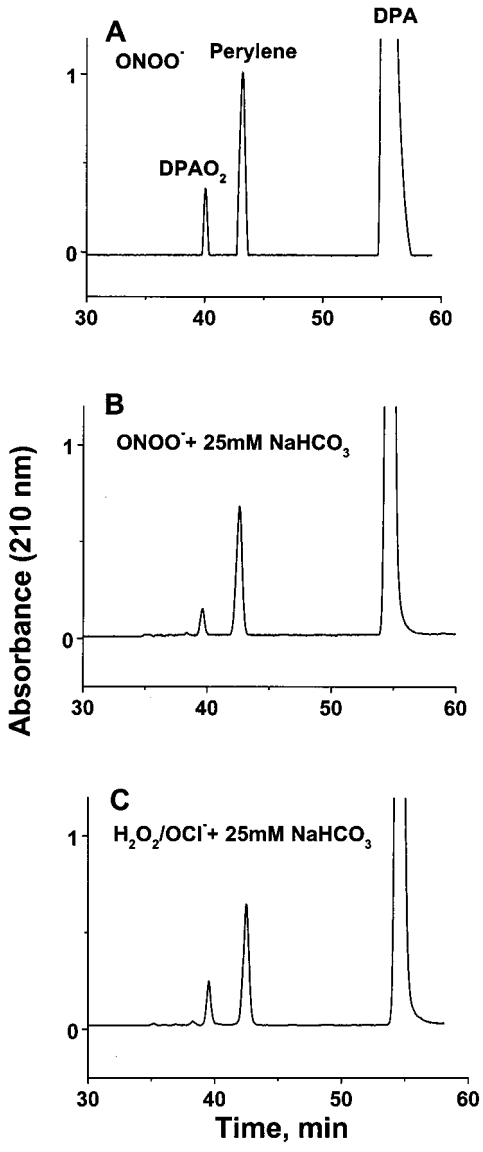

Fig. 4. Effect of $NaHCO_3$ on the generation of $^1O_2$ trapped by diphenylanthracene (DPA), thus generating diphenylanthracene endoperoxide ($DPAO_2$) in a CCl_4 layer after the decomposition of $ONOO^-$ in an aqueous layer in a biphasic system (see *Methods*). (*A*) Control experiment: HPLC elution profile of products after stepwise decomposition of $ONOO^-$ in the aqueous layer in the absence of TME in the CCl_4 layer (solution **A**; see *Methods*) and absence of $NaHCO_3$ in the aqueous layer. (*B*) Same as in *A*, but in the presence of 25 mM $NaHCO_3$ in the aqueous layer. *C* is the HPLC elution profile of a positive control experiment in which $^1O_2$ was generated from the highly efficient H_2O_2/OCl^- reaction in the aqueous layer containing 25 mM $NaHCO_3$. (For space consideration and because the 0- to 30-min profiles are without structures, the profiles are displayed only between 30 and 60 min).

sured by the $DPAO_2$/perylene, are compared in the HPLC elution profiles shown in Fig. 4 *A* and *B*. In Fig. 4*B*, depicting a typical result of a $OONO^-$ decomposition reaction in the presence of 25 mM sodium bicarbonate, the integrated area under the $DPAO_2$ elution trace is 15% of the area under the perylene standard elution trace whereas in the absence of bicarbonate this area is 30% (*A*). In Fig. 4*C*, in the H_2O_2/OCl^- reaction under analogous condition, this ratio is also 30%. Thus, in the H_2O_2/OCl^- reaction, the sodium bicarbonate seems to have no effect on the $^1O_2$ yield whereas this yield is decreased by $\approx$50% in the case of the $OONO^-$ decomposition to $^1O_2$ and NO^-; this result is consistent with the near-stoichiometric yield of nitrosylhemoglobin observed spectrophotometrically (Fig. 2).

Discussion

It is known that the final oxidation product of peroxynitrous acid, HOONO, is the isomeric nitric acid, HNO_3 (35). However, the intermediate steps leading to this end-product are not well known (22). Beckman *et al.* (18) proposed that HNO_3 is formed from a cascade of steps including the decomposition of HONOO to NO_2 and the ·OH radical, followed by a cage-mediated recombination of these two intermediates to form HNO_3, followed by deprotonation to NO_3^-. This mechanism is attractive because the ·OH radicals thus produced could account for the known oxidative properties of HOONO. However, the experimental evidence supporting an ·OH radical mechanism remains controversial (36, 37). Furthermore, Koppenol *et al.* (22) considered a variety of reaction mechanisms and primary decomposition products of $ONOO^-$ and concluded that the ·OH radical pathway was thermodynamically unfavorable. Instead, they proposed a new, strongly oxidizing intermediate, the vibra-

tionally excited trans-peroxynitrous acid. However, this interpretation was questioned, particularly the assumptions concerning the entropy of hydration of $ONOO^-$ (38).

It is instructive to review the known structural features of peroxynitrite before considering the possible decomposition mechanisms in more detail. Theoretical calculations suggest that the cis-configuration of $ONOO^-$ is favored over the trans-configuration (39). It has been shown recently by x-ray crystallography that peroxynitrite indeed crystallizes in the cis form (40). The ^{15}N-NMR data of Tsai *et al.* (39) also favors the cis-peroxynitrite form as the most stable and dominant isomer. The Raman spectrum of peroxynitrite in alkaline aqueous solution reveals an unusual broad band at 642 cm^{-1} that has been attributed to the $ONOO^-$ torsional motion of the cis-form (41). On the basis of this observation and other considerations, Tsai *et al.* concluded that the negative charge is delocalized over the entire planar cis-$ONOO^-$ molecule and that a weak hydrogen-bond-like interaction exists between the terminal oxygen atoms, thus forming a cyclic structure. The broadness of the 642 cm^{-1} band has been attributed to the heterogeneous interactions of the cis-$ONOO^-$ molecule with water molecules. Our results indicate that $ONOO^-$, upon protonation, decomposes into $^1O_2$ and NO^-. The proposed weakly bonded cis-cyclic structure of $ONOO^-$ (41) can serve as a basis of a model that can account for this observation. We recall the well known decomposition of the four-membered strained-ring triphenyl phosphite-ozone adduct that dissociates into $^1O_2$ via a spin-conserved process. In 1961, Thompson (42) reported that ozone and trialkyl phosphites form 1:1 adducts, which are stable at low temperatures (−78°C). Upon warming to −35°C, phosphates are produced, and molecular oxygen evolution is observed. On the basis of ^{31}P-NMR measurements, it was concluded that the precursor triphenyl phosphite-ozone adduct has a four-membered cyclic structure (42). Furthermore, based on the principle of spin-conservation, in 1964, Corey and Taylor suggested that the molecular oxygen evolved in this reaction is singlet molecular oxygen (43). In 1969, Murray and Kaplan for solution (44), and Wasserman *et al.* for the gas phase (45), confirmed the generation of singlet molecular oxygen in the thermal dissociation of triphenylphosphite-ozone adduct according to the following scheme:

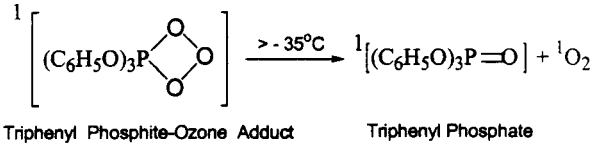

Proposed Ring Structure for Peroxynitrite. Based on the considerations outlined above, it is reasonable to propose that, in alkaline aqueous solution, the peroxynitrite anion exists also as a four-membered strained ring, the latter being stabilized by interactions with water molecules.[§] In this hypothesis (Fig. 5), the sum of the ring strain and the solvation free energy released on charge neutralization by protonation could provide the necessary energy for the generation of both the electronically excited $^1O_2$ and the ground state ^1HNO molecules (46). Because of the uncertainties associated with the thermodynamic parameters of $ONOO^-$ and related compounds (22, 38), a calculation associated with this reaction was not attempted here. A spin-conserved, acid-induced dissociation of peroxynitrite that generates $^1O_2$ predicts the simultaneous generation of a singlet nitroxyl species, ^1HNO, which deprotonates to form NO^- at pH

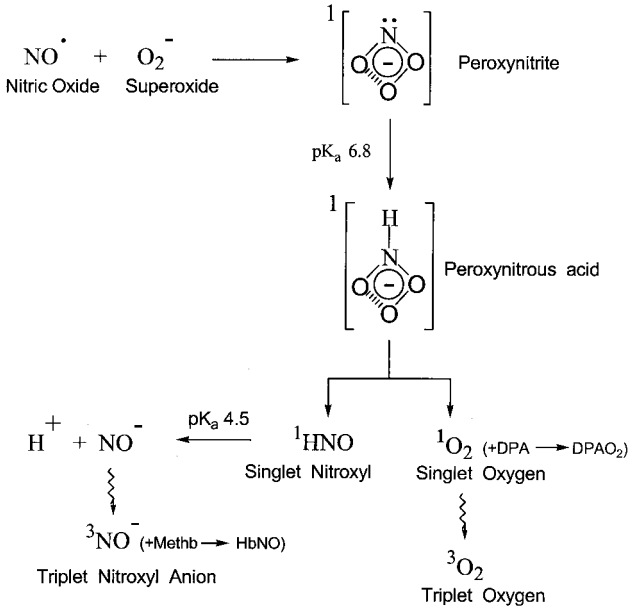

Fig. 5. Proposed strained 4-membered ring structure of peroxynitrite anion, its protonation, and proposed spin-conserved decomposition of peroxynitrous acid at pH 7, thus generating the transient reactants, ground state ^1HNO, and electronically excited $^1O_2$. The NO^-, formed by the deprotonation of ^1HNO, is trapped by MetHb to form nirosylhemoglobin (HbNO). The $^1O_2$ formed was trapped by diphenylanthracene (DPA) to form the stable (at room temperature) endoperoxide $DPAO_2$.

7.0 because the pKa of HNO is 4.7 (47). The nitroxyl anion was trapped by MetHb to generate nitrosyl hemoglobin, HbNO. From Fig. 2, it is evident that the HbNO complex formation approaches saturation when the estimated $OONO^-$ concentration is equal to the MetHb concentration (Fig. 2). This suggests that a 1:1 complex of NO^-:MetHb is formed and that the production of NO^- from $OONO^-$ occurs in high yield, as observed previously in the decomposition of Angeli's salt into NO^- trapped by MetHb (28).

Interaction of Peroxynitrite Anion with Bicarbonate. Based on the kinetics of decay of peroxynitrite in the presence of sodium bicarbonate as a function of pH, Lymar and Hurst showed that dissolved CO_2 enhanced the rate of decay of peroxynitrite (19). They proposed that an adduct $ONOOCO_2^-$ is formed as a result and that the decomposition pathways of this adduct are different from those of $ONOO^-$ (48, 49). The details of the mechanisms of decomposition of the $ONOOCO_2^-$ complex are not well understood (49). Our results show that, in the presence of HCO_3^-, the singlet oxygen trapping yield is decreased (Fig. 4). However, the results of the NO^- trapping experiments by MetHb suggest that the concentration of NO^- released by the decomposition of $ONOO^-$ in the presence of 25 mM $NaHCO_3$ is not significantly affected (Fig. 2). This suggests that, within the decomposing intermediate $ONOOCO_2^-$ complex (19), the electronically excited $^1O_2$ state is quenched and therefore the yield of $DPAO_2$ is diminished (Fig. 4). However, the concentration of NO^- arising from the deprotonation of ground state ^1HNO should remain unaffected, as observed experimentally (Fig. 2). Because bicarbonate is in equilibrium with CO_2 in aqueous solutions, and because CO_2 is not a quencher of $^1O_2$ (50), the diminished yield of $DPAO_2$ may arise from the interaction of $^1O_2$ with HCO_3^-. However, this latter reaction has not yet been characterized.

[§]As suggested by a referee, it is conceivable that further research (e.g., by isotope labeling of oxygen, ^{18}O or ^{17}O) could establish whether the cyclic structure is a transition state or a stable intermediate.

Unimolecular Isomerization of Peroxynitrite to Nitrate Ion. On the basis of previous thermodynamic and kinetic studies, it has been proposed that peroxynitrous acid, HOONO, isomerizes unimolecularly to HNO_3, thus giving rise to the ultimate product NO_3^- (22). However, our results suggest that NO^- is implicated in the ultimate formation of NO_3^-. In support of this suggestion, we recall that (*i*) NO^- is quite easily oxidized in solution to NO by $^3O_2$ and a variety of biological oxidants (51), and (*ii*) Ignarro *et al.* (52) have shown that, in aerobic aqueous solution, NO is first oxidized to nitrite (NO_2^-), and then to the NO_3^- ion. Oxidation of NO_2^- to NO_3^- requires the presence of additional oxidizing species.

The role of peroxynitrite *in vivo* is based largely on the detection of 3-nitrotyrosine in animal tissue inflammation (53). It is not yet known whether the mechanism of decomposition of $ONOO^-$ to NO^- and $^1O_2$ is operative in physiological systems or leads to the nitration of tyrosine or to DNA damage (54). Wogan and coworkers (17) have shown that $ONOO^-$ is mutagenic in the *supF* shuttle vector pS189 in bacteria or human cells; the mutational spectra induced by peroxynitrite are similar to the mutational patterns induced by $^1O_2$. They suggested that genotoxic derivatives of peroxynitrite are likely to include species that have DNA-damaging properties resembling those of $^1O_2$ in selectivity. Finally, macrophages and neutrophils are known sources of O_2^- and NO (2–4), hence of peroxynitrite as well. Steinbeck *et al.* (27, 55) have shown that macrophages and neutrophils indeed generate singlet oxygen in significant amounts, comparable to the amount of oxygen consumed in a respiratory burst.

The authors are deeply indebted to Dr. Thérèse Wilson for her interest in this research, her encouragement, and numerous stimulating discussions. The authors are also grateful to Olga Rechkoblit for her assistance. This project was supported by a grant from the New York University Research Challenge Fund and by a grant from the Kresge Foundation.

1. Huie, R. E. & Padmaja, S. (1993) *Free Radical Res. Commun.* **18,** 195–199.
2. Marletta, M. A., Yoon, P. S., Leaf, C. D. & Wishnok, J. S. (1988) *Biochemistry* **27,** 8706–8711.
3. Xia, Y & Zweier, J. L. (1997) *Proc. Natl. Acad. Sci. USA* **94,** 6954–6958.
4. McCall, T. B., Boughton-Smith, N. K., Palmer, R. M. J., Whittle, B. J. R. & Moncada, S. (1989) *Biochem. J.* **261,** 293–296.
5. Ignarro, L. J., Buga, G. M., Wood, K. S., Byrns, R. E. & Chaudhuri, G. (1987) *Proc. Natl. Acad. Soc. USA* **84,** 9265–9269.
6. Vasquez-Vivar, J., Kalyanaraman, B., Martasek, P., Hogg N., Masters, B. S. S., Karoui, H., Torodo, P. & Pritchard, K. A. (1998) *Proc. Natl. Acad. Sci. USA* **95,** 9220–9225.
7. Ischiropoulous, H., Zhu, L. & Beckman, J. S. (1992) *Arch. Biochem. Biophys.* **298,** 446–451.
8. Carreras, M. C., Pargament, G. A., Catz, SD, Poderoso, J. J. & Boveris, A. (1994) *FEBS Lett.* **341,** 65–68.
9. Xia, Y., Dawson, V. L., Dawson, T. M., Snyder, S. H. & Zweier, J. L. (1996) *Proc. Natl. Acad. USA.* **93,** 6770–6774.
10. Feig, D. I., Reid, T. M. & Loeb, L. A. (1994) *Cancer Res.* **54,** Suppl., 1890s–1894s.
11. White, R. C., Brock, T. A., Chang, L., Crapo, J., Brisco, P., Ku, D., Bradley, W. A., Gianturco, S. H., Gore, J., Freeman, B. & Tarpey, M. M. (1994) *Proc. Natl. Acad. Sci. USA* **91,** 1044–1048.
12. Oury, T. D., Piantadosi, C. L. & Crapo, J. D. (1993) *J. Biol. Chem.* **268,** 15394–15398.
13. Beckman, J. S., Carson, M., Smith, C. D. & Koppenol, W. H. (1993) *Nature (London)* **364,** 584.
14. Pryor, W. & Squadrito, G. L. (1995) *Am. J. Physiol.* **268,** L699–L722.
15. Radi, R., Beckman, J. S., Bush, K. M. & Freeman, B. A. (1991) *Arch. Biochem. Biophys.* **288,** 481–487.
16. Ischiropoulous, H. & Al-Mehdi, A. B. (1995) *FEBS Lett.* **364,** 279–282.
17. Jeong, J. K., Juedes, M. J. & Wogan, G. N. (1998) *Chem. Res. Toxicol.* **11,** 550–556.
18. Beckman, J. S., Beckman, T. W., Chen, J., Marshall, P. A. & Freeman, B. A. (1990) *Proc. Natl. Acad. Sci. USA* **87,** 1620–1624.
19. Lymar, S. V. & Hurst, J. K. (1995) *J. Am. Chem. Soc.* **117,** 8867–8868.
20. Marnett, L. J. (1998) *Chem. Res. Toxicol.* **11,** 709–721.
21. Fukuto, J. M. & Ignarro, L. G. (1997) *Acc. Chem. Res.* **30,** 149–152.
22. Koppenol, W. H., Moreno, J. J., Pryor, W. A., Ischiropoulos, H. & Beckman, J. S. (1992) *Chem. Res. Toxicol.* **5,** 834–842.
23. Khan, A. U. (1995) *J. Biolumin. Chemilumin.* **10,** 329–333.
24. Held, A. M., Halko, D. J. & Hurst, J. K. (1978) *J. Am. Chem. Soc.* **100,** 5732–5740.
25. Wasserman, H. H., Scheffer, J. R. & Cooper, J. L. (1972) *J. Am. Chem. Soc.* **94,** 4991–4996.
26. Turro, N., Chow, M.-F. & Rigaudy, J. (1981) *J. Am. Chem. Soc.* **103,** 7218–7224.
27. Steinbeck, M. J., Khan, A. U. & Karnovsky M. J. (1992) *J. Biol. Chem.* **267,** 13425–13433.
28. Bazylinski, D. A. & Hollocher, T. C. (1985) *J. Am. Chem. Soc.* **107,** 7982–7986.
29. Hughes, M. N. & Nicklin (1968) *J. Chem. Soc. A* 450–452.
30. Wang, J. H. (1962) in *Oxygenases*, ed. Hayaishi, O. (Academic, New York), p. 472.
31. Kern, C. E. (1960) *J. Chem. Educ.* **37,** 14–23.
32. Antonini, E. & Brunori, M. (1971) *Hemoglobin and Myoglobin in Their Reactions with Ligands* (North–Holland, Amsterdam).
33. Wilkinson, F. & Brummer, J. G. (1981) *J. Phys. Chem. Ref. Data* **10,** 809–999.
34. Koo, J. & Schuster, G. B. (1978) *J. Am. Chem. Soc.* **100,** 4496–4503.
35. Ray, J. D. (1962) *J. Inorg. Nucl. Chem.* **24,** 1159–1162.
36. Moreno, J. J. & Pryor, W. A. (1992) *Chem. Res. Toxicol.* **5,** 425–431.
37. Van der Vilet, A., O'Neil, C. A., Halliwell, B., Cross, C. E. & Kaur, H. (1994) *FEBS Lett.* **339,** 89–92.
38. Merenyi, G. & Lind, J. (1997) *Chem. Res. Toxicol.* **10,** 1216–1220.
39. Tsai, H., Hamilton, T. P., Tsai, J. M., van der Woerd, M., Harrison, J. G., Jablonsky, M. J., Beckman, J. S. & Koppenol, W. H. (1996) *J. Phys. Chem.* **100,** 15087–15095.
40. Worle, M., Latal, P., Kissner, R., Nesper, R. & Koppenol, W. H. (1999) *Chem. Res. Toxicol.* **12,** 305–307.
41. Tsai, J. M., Harrison, J. G., Martin, J. C., Hamilton, T. P., van der Woerd, M., Jablonsky, M. J. & Beckman, J. S. (1994) *J. Am. Chem. Soc.* **116,** 4115–4116.
42. Thompson, Q. E. (1961) *J. Am. Chem. Soc.* **83,** 845–851.
43. Corey, E. J. & Taylor, W. C. (1964) *J. Am. Chem. Soc.* **86,** 3881–3882.
44. Murray, R. W. & Kaplan, M. L. (1969) *J. Am. Chem. Soc.* **90,** 537–538.
45. Wasserman, E., Murray, R. W., Kaplan, M. L. & Yager, W. A. (1969) *J. Am. Chem. Soc.* **90,** 4160–4161.
46. Wu, A. A., Peyerimhoff, S. D. & Buenker, R. J. (1978) *Chem. Phys. Lett.* **35,** 316–322.
47. Gratzel, M., Taniguchi, S. & Henglein, A. (1970) *Ber. Bunsenges. Phys. Chem.* **74,** 1003–1010.
48. Uppu, R. M., Squadrito, G. L. & Pryor, W. A. (1996) *Arch. Biochem. Biophys.* **327,** 335–343.
49. Bartberger, M. D., Olson, L. P. & Houk, K. N. (1998) *Chem. Res. Toxicol.* **11,** 710–711.
50. Ogryzlo, E. A. (1979) in *Singlet Oxygen*, eds. Wasserman, H. H. & Murray, R. W. (Academic, New York), pp. 35–58.
51. Fukuto, J. M., Hobbs, A. J. & Ignarro, L. J. (1993) *Biochem. Biophys. Res. Commun.* **196,** 707–713.
52. Ignarro, L. J., Fukuto, J. M., Griscavage, J. M., Rogers, N. E. & Byrns, R. E. (1993) *Proc. Natl. Acad. Sci. USA* **90,** 8103–8107.
53. Kooy, N. W., Lewis, S. J., Royall, J. A., Ye, Y. Z., Kelly, D. R. & Beckman, J. S. (1997) *Crit. Care Med.* **25,** 812–819.
54. Burney, S., Caulfield, J. L., Niles, J. C., Wishnok, J. S. & Tannenbaum, S. R. (1999) *Mutat. Res.* **424,** 37–49.
55. Steinbeck, M. J., Khan, A. U. & Karnovsky M. J. (1993) *J Biol Chem* **268,** 15649–15654.